Cryotherapy for Breast Fibroadenomas[1]

Peter J. Littrup, MD
Laurie Freeman-Gibb, RN, NP
Aleodor Andea, MD
Michael White, MD
Kathy Carolin Amerikia, MD
David Bouwman, MD
Ted Harb, MD
Wael Sakr, MD

Published online before print
10.1148/radiol.2341030931
Radiology 2005; 234:63–72

[1] From the Departments of Radiology (P.J.L., T.H.), Surgery (M.W., K.C.A., D.B.), and Pathology (A.A., W.S.), and the Karmanos Cancer Center (L.F.G.), Wayne State University School of Medicine, Harper University Hospital, 3990 John R St, Detroit, MI 48201. Received June 19, 2003; revision requested August 27; final revision received August 11, 2004; accepted August 16. Supported in part by a grant from Sanarus Medical, who provided professional and technical fees and equipment free of charges. **Address correspondence to** P.J.L. (e-mail: *peterlittrup@aol.com*).

Author contributions:
Guarantors of integrity of entire study, P.J.L., L.F.G.; study concepts, P.J.L., L.F.G., M.W.; study design, P.J.L., L.F.G., A.A., M.W., W.S.; literature research, P.J.L., T.H.; clinical studies, P.J.L., L.F.G., M.W., K.C.A., D.B., W.S.; data acquisition, all authors; data analysis/interpretation, P.J.L., L.F.G., A.A., W.S.; statistical analysis, P.J.L.; manuscript preparation, P.J.L., L.F.G.; manuscript definition of intellectual content, P.J.L.; manuscript editing, P.J.L., L.F.G., K.C.A., D.B., T.H., W.S.; manuscript revision/review, P.J.L., L.F.G., A.A.; manuscript final version approval, all authors

PURPOSE: To assess freezing protocols, imaging, and clinical outcomes of percutaneous ultrasonographically (US)-guided cryotherapy for breast fibroadenomas.

MATERIALS AND METHODS: Institutional review board approval and patient consent were obtained. Forty-two biopsy-confirmed fibroadenomas were treated in 29 patients (mean age, 27 years) by using a 2.4-mm cryoprobe inserted into the fibroadenoma with US guidance. The first seven patients underwent conscious sedation, but the other 22 patients required only local anesthesia. US and thermocouple monitoring of the procedure were performed to evaluate freeze protocols based on tumor size. Saline injections protected the skin and/or chest wall. US follow-up was performed at 1 week and at 1, 3, 6, and 12 months. Pre- and 12-month postcryotherapy mammograms were available for seven patients who were over 30 years old. χ^2 and Student t tests were used to assess frequency and mean differences, respectively.

RESULTS: The 22 patients who underwent local anesthesia reported minimal discomfort. No significant complications were noted, and patients were very pleased with the resolution of palpable mass effect and cosmetic results. The average pretreatment fibroadenoma volume of 4.2 $cm^3 \pm$ 4.7 (standard deviation) was reduced to 0.7 $cm^3 \pm$ 0.8 at 12-month follow-up (73% reduction, $P < .001$). US produced excellent ice visualization beyond tumor margins, while thermocouples confirmed cytotoxic temperatures approximately 5 mm behind the visible leading edge. Two patients elected to undergo either removal or biopsy of a residual mass, which revealed a shrunken hyaline matrix with preserved collagenous architecture. Mammograms showed comparable resolution of mass effects with mild surrounding parenchymal reaction.

CONCLUSION: Cryotherapy of fibroadenomas is a safe, effective, and virtually painless clinic-based (ie, outpatient) treatment option with good cosmesis.

Nonsurgical treatments for benign breast masses have clinical goals of stopping growth and/or reducing (removing) palpable mass effect without leaving a surgical scar (ie, good cosmesis). If cryotherapy could accomplish these goals, substantial psychologic and economic benefits could be realized for many of the 1.3 million women who undergo breast biopsy each year in the United States (1). Despite the increasing use of confirmatory needle biopsy, an estimated 500 000 fibroadenomas are still surgically excised (2,3). Factors that may lead patients to choose removal of a benign mass include palpable prominence, localized discomfort, interval growth, and peace of mind. For certain patient groups, multiple growing masses are more problematic. Fibroadenomas in African American women occur at a younger age, are more commonly multiple, and overall have twice the incidence of those seen in white women (4–7).

Resection has been the standard, but nonsurgical options for benign or malignant breast masses include vacuum-assisted biopsy (8,9), radiofrequency ablation (10,11), laser therapy (12), and cryotherapy (2,3,13,14). Newer 8-gauge vacuum-assisted biopsy devices may achieve visual removal for some masses up to 2 cm in maximal diameter, but complete resection may still be limited by targeting and/or visualization difficulties due to local hemorrhage as multiple cores are obtained (9). Heat-based treatments are difficult to monitor with ultrasonography (US) and are limited by potential skin damage if masses are less than 1 cm from the chest wall or skin surface (11). Cryotherapy is easily visualized with

high-frequency (ie, high-spatial-resolution) US as the ice margin extends beyond the tumor, is virtually painless, and can be used for masses near the skin. In this article we describe the experience of the single institution with the largest cohort and focus on its unique detailed imaging database, which was not covered in the article from the multicenter trial (2,3), and share some insights from our patient population. The purpose of our study was to assess freezing protocols, imaging, and clinical outcomes of percutaneous US-guided cryotherapy for breast fibroadenomas.

MATERIALS AND METHODS

Patients

Procedures were performed under an instutional review board–approved protocol as part of a multicenter prospective trial. An informed consent form for the trial was also approved by our institutional review board and was thoroughly discussed with and signed by all patients. This report is limited to the institution at which more than 50% of cases in that trial were performed (2,3), with collection of detailed imaging aspects of freeze monitoring and evaluation over time. Prior to cryotherapy, large-core needle biopsy was performed to confirm the diagnosis of 42 fibroadenomas in 29 patients. All biopsy and cryotherapy procedures were performed by a radiologist (P.J.L.) with approximately 10 years of interventional and breast imaging experience. The consecutive patients who met our study criteria were newly diagnosed, had growing fibroadenomas or palpable discomfort, and were offered resection in all cases. A growing fibroadenoma was defined by an increase in at least two of three dimensions on breast US images. Age and race were assessed in relation to outcomes. The first seven procedures were performed as ambulatory surgery and made use of intravenous sedation. It quickly became apparent that an office (outpatient) setting and local anesthesia without sedation were more appropriate for the procedure, so all subsequent cases were performed in such a manner.

Equipment and Cryotherapy Protocols

Real-time US guidance was used to document fibroadenoma sizes and to guide thermocouple and probe placements, as well as to monitor iceball formation and associated safety measures (ie, sterile saline injections). US monitoring (model 9000; GE Medical Systems, Milwaukee, Wis) was performed (P.L.L., approximately 10 years of experience in US guidance) with a high-frequency (10–13 MHz) linear-array probe. Each fibroadenoma was characterized with respect to its general location within the breast (ie, quadrant) and its width, height, and length. Note was also made of tumor blood supply by using power Doppler estimates of internal, or "feeder," vascularity.

During the freeze cycles, the maximal transverse dimension of the iceball was recorded for each minute of the freeze and refreeze cycles. Longitudinal iceball measurements do not change significantly during freezes along the 4-cm exposed tip; therefore, overall ice lengths were consistently 5–6 cm for all freezes. The iceball size at the initiation of the second freeze was back-calculated by using the stable rates of iceball progression (in centimeters per minute). A disposable 2.4-mm–diameter air-gap–insulated cryoablation probe (Visica Treatment System; Sanarus Medical, Pleasanton, Calif) was used for all masses. In 10 cases, a multiple port system (Cryocare; Endocare, Irvine, Calif) was used so that two probes could be used simultaneously, as follows: In nine patients, two masses were treated at the same time, and in one patient, two probes were used to cover a larger discoid mass ($3.9 \times 3.9 \times 1.3$ cm) for which the long axis of the cryoablation probe simply could not be chosen for the greatest fibroadenoma measurement. Freezing at the distal end of the cryoprobe occurred according to the Joule-Thompson effect, in which argon gas is decompressed by more than 2000 psi (14 000 kPa) within the closed tip of the probe, reaching temperatures approaching that of liquid argon (−187°C).

The Visica Treatment System and Cryocare units have adjustable duty cycles, which can be used to alter the length of time that argon gas expands to cool the probe. At "100% duty cycle" argon flows continuously, while at "10% duty cycle" argon flows for 1 second and is stopped for 9 seconds of every 10-second period. We decided that protocol freeze parameters needed to be altered after our first case, in which we used a 100% freeze for 10 minutes, followed by a 10-minute thaw and another 10-minute 100% freeze. The resultant iceball dimensions ($3.5 \times 3.5 \times 5.5$ cm) were considered too destructive for the surrounding normal tissue in the treatment of most benign tumors (ie, <2 cm in average diameter). A balance of sufficient freeze time and intensity was standardized according to the size of fibroadenomas, which were grouped by 1-cm increments up to 4 cm, at all investigational sites (2,3). The freeze times were selected according to the algorithm to accommodate the greatest dimension of fibroadenoma sizes for each of four maximum tumor diameter ranges (protocols 1–4: 0–1.0 cm, 1.1–2.0 cm, 2.1–3.0 cm, and 3.1–4.0 cm, respectively) within the relatively insulating (ie, fatty) breast tissues. The problem of inadequate treatment was prevented by limiting maximal fibroadenoma dimension to 4 cm, which also helped avoid the problem of phyllodes tumors, which are rarely smaller than 4 cm (2–6). In addition, if thorough coverage by toxic ice (ie, <−40°C) is achieved, even locally aggressive higher-Gleason-score prostate tumors have shown potentially better long-term outcomes than has surgery or radiation therapy (14).

At our investigational site, we also elected to obtain thermocouple documentation of cytotoxic temperature margins within the breast tissues. For all tumors 1 cm in diameter or larger, each 100% duty cycle freeze was followed by a maintenance freeze at 10% duty cycle; this process was designed to maintain cold temperatures within the tumor while slowing the expansion of the iceball beyond its borders. Osmotic shifts take place during thawing (15,16), which sensitize cells for greater cytotoxicity during the second freeze. Therefore, a freeze-thaw-freeze technique was used in all cases. The passive thaw between the first and second freeze was continued until the probe warmed to about −1°C. Typically, the time required for such warming was about the same as the total time of each freeze.

Procedure

The patients were prepped and draped in sterile fashion. The angle of approach was chosen along the longest axis of the fibroadenoma to use the longer freeze length of the cryoprobe. A lateral or inferior puncture site was selected when possible for best cosmetic results. The overlying skin was infiltrated with buffered 2% lidocaine and was extended around all tumor margins. After a 3-mm skin nick was made, a 12-gauge coaxial trocar needle (Bard, Covington, Ga) was advanced through the center of the fibroadenoma. Transverse US scanning (Fig 1a) allowed us to verify central placement. Once the trocar needle tip penetrated the distal margin of the mass (Fig 1b), the stylet was removed and was replaced with the 2.4-mm cryoprobe. The needle sheath was then retracted to ex-

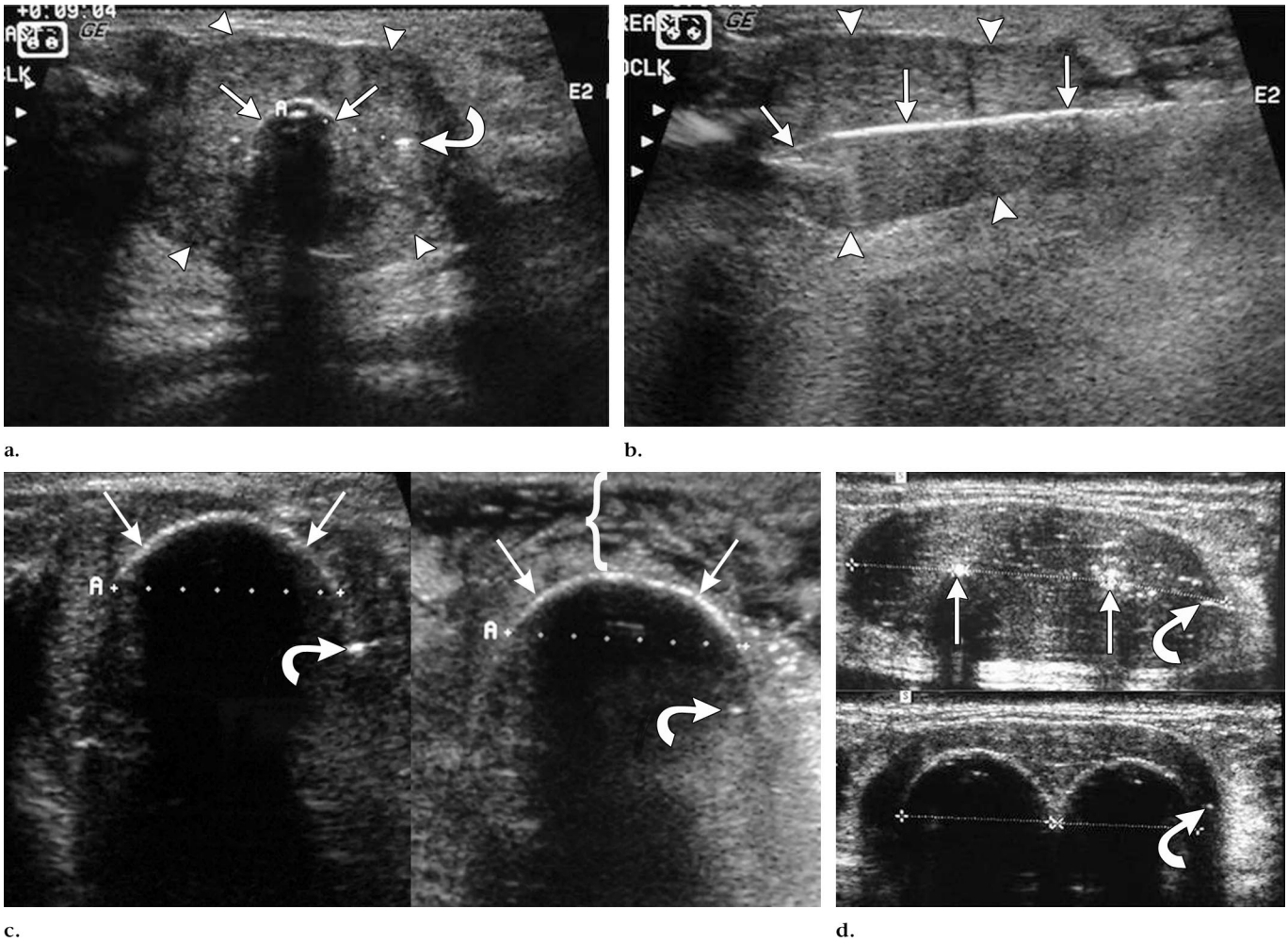

Figure 1. US images. **(a)** Transverse view of developing iceball (<1 cm in diameter; straight arrows) in 2.3-cm-diameter fibroadenoma (arrowheads) at initiation of freeze. Thermocouple tip (curved arrow) is 7 mm from the cryoprobe. **(b)** Longitudinal view of fibroadenoma (arrowheads) with a 12-gauge trocar placement needle (arrows) prior to removal of the stylet and replacement with the cryoprobe. **(c)** Transverse view of growing iceball (straight arrows) at 2 (left) and 3 (right) minutes, and thermocouple (curved arrow) is just becoming engulfed in ice at 6°C and −6°C, respectively. At 3 minutes, note the thickened skin distance (bracket) due to interval saline injection. **(d)** Transverse view of a large unusually shaped (ie, discoid, not cylindrical) fibroadenoma with cryoprobes (straight arrows) in place (top) and growing ice at 1 minute (bottom). The thermocouple (curved arrow) is about to be engulfed in ice. The iceball subsequently fused to create a smooth discoid shape, which was only possible with the probes placed less than 1.5 cm apart and approximately 1 cm from the fibroadenoma margin.

pose the distal 4 cm of the cryoprobe. The coaxial sheath also helped insulate the insertion tract from freezing damage. The system was then briefly activated at 10% duty cycle to "stick freeze" the probe in place, while a thermocouple was placed through an 18-gauge arterial needle. The thermocouple tip was lodged beneath the outer rim of the fibroadenoma, which prevented it from subsequently being pushed laterally by the advancing iceball in the loose breast fat (Fig 1c, 1d). Thermocouple distance from the cryoprobe varied between 4 and 12 mm, depending on the fibroadenoma diameter and the depth of insertion of the thermocouple beneath the capsule. Temperatures from thermocouples within the fibroadenoma and along the skin surface were recorded at 1-minute increments throughout the procedure.

At the time of this trial, cryoprobes had air-gap insulation and allowed freezing temperatures to propagate up the probe shaft. Skin protection at the cryoprobe insertion site included the dripping of sterile room-temperature saline on the skin and the placement of moist gauze between the probe (or sheath) and the skin. US-guided sterile saline injections (range, 10–40 mL) were used between the iceball and the skin surface (Fig 2) or chest wall, when needed, throughout both freeze cycles to keep the advancing ice at least 5 mm from either surface. In later patients (ie, later in consecutive enrollement), saline injection was not necessary between the iceball and chest wall as long as gentle to-and-fro movement of the iceball within the breast was maintained. This motion prevented ice from propagating posteriorly but needed to be initiated before the ice margin came close to the pectoralis muscle.

Switching from argon to helium gas by means of the thaw switch on the systems actively warmed the probe after the final freeze cycle. This "active thawing" phenomenon facilitated prompt removal (ie, <2 min) of the probe from the iceball. Manual pressure was then applied for at least 20 minutes to decrease the risk of hematoma formation. Patients were discharged home with a pain scale question-

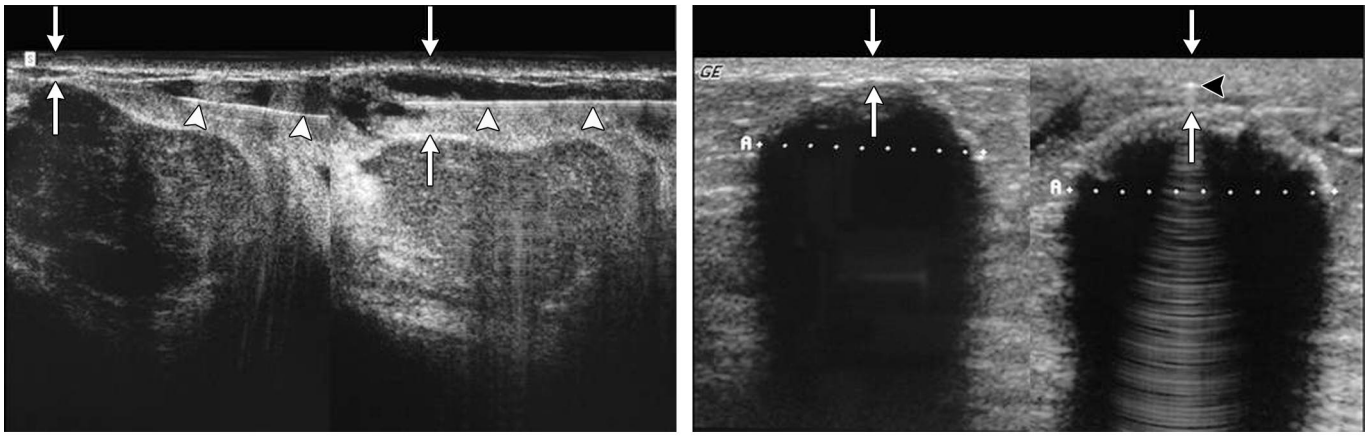

a. **b.**

Figure 2. **(a)** Longitudinal and **(b)** transverse US views show progress of saline injection. The needle (arrowheads) is increasing the distance (arrows) from the skin surface to the fibroadenoma, from less than 3 mm (left image in both **a** and **b**) to more than 8 mm (right image in both **a** and **b**).

naire to monitor any discomfort. A standard visual analog pain scale (ie, score of 0–10, corresponding to a spectrum of facial expressions from happy [score of 0] to crying [score of 10]) was used. Patients were seen at follow-up at 1 and 6 weeks and at 3, 6, and 12 months after cryotherapy in our comprehensive breast center.

At follow-up, patient satisfaction, tumor palpability, and clinical appearances were evaluated by a single nurse practitioner (L.F.G.) with approximately 10 years of dedicated breast care experience at our center. She monitored overall patient well-being (eg, constitution, affect), as well as palpably measured mass effect (ie, estimate of outer fibroadenoma margins in centimeters) and clinical appearance related to skin appearance and/or scarring. All US images and available mammograms ($n = 7$) were evaluated by an experienced breast imager (P.J.L.). Margins of treatment effect in adjacent tissues and the underlying fibroadenoma were both measured on US images, and the overall appearance (eg, cystic component, vascular flow) was noted. Since the number of follow-up mammograms was too limited for any significant analysis, overall appearance (ie, visibility and/or size of fibroadenoma mass effect and density of surrounding parenchyma) was noted. Three patients underwent follow-up biopsy because of their concern and/or dissatisfaction about persistent or perceived increase in palpable mass effect. Specimens were evaluated by a pathologist (W.S.) with approximately 15 years of breast pathology expertise.

Statistical Analysis

Assessment was limited to observational differences and was not intended to power the sample size of the study. The two-tailed Student *t* test was used for all mean value comparisons. The χ^2 test was used for frequency comparisons (ie, percentages). A significant difference was declared at $P < .05$. Analyses were performed by the lead author (P.J.L.) by using calculated fields on a standard spreadsheet (Excel; Microsoft, Redmond, Wash) and were validated by the sponsoring company (Sanarus Medical).

RESULTS

Twenty-nine patients underwent cryoablation of 42 fibroadenomas. Nine patients had two fibroadenomas treated in one session and 19 had a single fibroadenoma treated. One 15-year-old white patient who had undergone four previous resections and had associated keloid scarring underwent three cryotherapy sessions for five new fibroadenomas treated within this protocol, and the sessions were performed approximately 3 months apart. She also had two additional fibroadenomas treated off-protocol (ie, not included in this study) following U.S. Food and Drug Administration approval of the procedure and coverage by her insurance. African American patients comprised the majority of the study group (16 of 27, 60%). Patient age ranged from 13 to 50 years (mean, 26.6 years); African American ($n = 16$) and non–African American ($n = 11$) patients had mean ages of 24.6 years ± 11.9 (± standard deviation) and 29.0 years ± 11.9, respectively. There was no statistically significant difference in the mean age by race nor was there any significant racial predilection for other outcome parameters ($P > .05$). A total of 37 fibroadenomas had at least 1 year of follow-up. Because of the young age of most patients, only seven women (over 30 years of age) underwent pre- and postprocedure mammography. Patient-reported pain on the visual analog scale averaged a score of only 1 (out of 10) during the first week, then pain resolved. The average pretreatment fibroadenoma volume of 4.2 cm^3± 4.7 was markedly reduced to 0.7 cm^3± 0.8 at 12 months (73% reduction, $P < .001$).

US and Temperature Monitoring

Rapid iceball growth occurred with the initial 100% duty cycle at an estimated rate of 1.2 cm/min for the first minute and then slowed to approximately 0.3 cm/min for the next 3 minutes for all protocols (Fig 3). The 10% "maintenance" freeze slowed the rate of iceball expansion to less than 0.1 cm/min. During the thaw phase, the iceball diameter reduced approximately 7–8 mm in all protocols. During the second freeze, progression of iceball size during the 100% duty cycle was approximately 0.4 cm/min for protocol 2 but was only 0.15 cm/min for protocols 3 and 4. Slowing of the iceball progression at 10% duty cycle in the second freeze (0.075 cm/min) occurred promptly for protocol 2 but appeared delayed by 1 and 2 minutes for

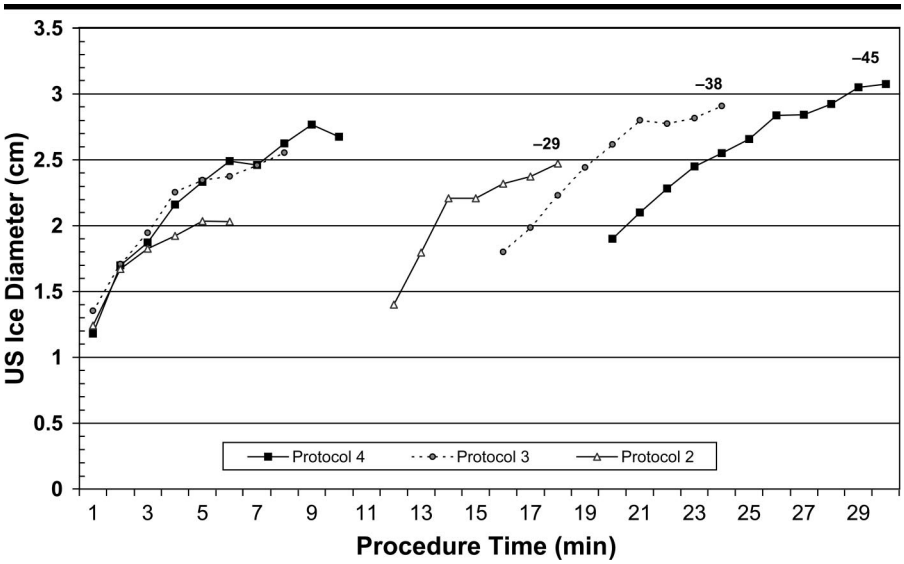

Figure 3. Graph shows transverse iceball dimensions over time for three freeze protocols, as well as lowest mean temperature attained at completion of second freeze. The two sets of ice growth curves correspond to the freeze portions with intervening thaw, which shows that small tumors were treated within about 18 minutes whereas the largest tumors took about 30 minutes total. *Protocol 2* (1.1–2.0-cm fibroadenoma) = 2 minutes at 100%, 4 minutes at 10%; *Protocol 3* (2.1–3.0-cm fibroadenoma) = 4 minutes at 100%, 4 minutes at 10%; *Protocol 4* (>3-cm fibroadenoma) = 4 minutes at 100%, 6 minutes at 10%.

protocols 3 and 4, respectively. The second freeze cycle expanded the freeze rim approximately 5 mm beyond the greatest extent achieved at the conclusion of the first freeze for all protocols. At the end of the second freeze, no differences in mean iceball diameter were noted between protocols 2 and 3 (approximately 2.0 vs 2.4 cm, respectively; $P < .05$) than between protocols 3 and 4 (approximately 2.4 vs 2.6 cm).

Cytotoxic tissue temperatures (<−20°C) were noted at the periphery of the iceball at the completion of the second freeze for all protocols. Average final temperatures were used to avoid inherent measurement errors with thermocouple placements and their associated variable distances from the cryoprobe. Lower temperatures were noted for longer freeze times, which suggests that while the iceball may not grow significantly after a stabilization phase, the cytotoxic isotherm continues to move closer to the visualized ice margin over time. From these observations, a uniformly cytotoxic temperature of less than −40°C (14–16) appeared to lay approximately 5 mm behind the leading edge of the visualized iceball at the second freeze. Total procedure times were not specifically measured, but Figure 3 confirms that the actual total time for freezing cycles and probe removal is less than 30 minutes.

Follow-up Imaging and Clinical and Pathologic Evaluation

The change in US appearance over time provided both qualitative and quantitative information about the healing phases of breast cryoablation. By the end of the second freeze, ice margins extended beyond the fibroadenoma margins in all patients. This was substantiated by noting the evolving US appearance of the fibroadenoma and adjacent breast tissue during follow-up (Fig 4). Color Doppler flow was not seen within the treatment zone but appeared more intense immediately beyond the echogenic cryoablation margin during the first week after ablation. Color Doppler evaluation at later follow-up still showed no significant flow in the cryoablation zone and showed more normalized flow in adjacent tissue. After 3 months, differentiation of the ablated fibroadenoma from the surrounding treated area at US became more difficult in some patients. At 6 months, four fibroadenomas showed some fragmentation, one of which had a cystic component. At 12 months, continued shrinkage occurred to the point that five of the fibroadenomas could no longer be identified, and 10 were reduced by more than 90% in volume.

A potentially aberrant healing reaction in the surrounding parenchyma occurred in three younger patients and was therefore seen only at US (Fig 5). At 6 months, a palpably soft but larger area was noted at physical examination and US of the treatment site. The region had overall echotexture similar to that of hypoechoic breast fat, including subtle structural bands. While no significant color Doppler flow was noted in the central fibroadenoma scar, normal color Doppler flow was noted within this surrounding region. One patient elected to continue conservative observation with US. One patient elected to undergo resection of the whole area, and another underwent large-core needle biopsy of the peripheral and central areas. Histologic results are available from these two cases of periablation tissue reaction (Fig 5), as well as from the single case in which a patient requested excision for suboptimal tumor volume reduction, despite a decrease from 2.0 to 0.7 cm^3 (70% reduction). In all three of these cases, histologic results from the fibroadenoma scar revealed extremely hypocellular or acellular collagenized stroma with very few or absent epithelial components. The two excision specimens demonstrated close size correlation with that seen on the US image of the shrunken scar (Fig 5d). In all three cases, peripheral histologic evaluation revealed normal breast tissue (Fig 5c). In the case of the dissatisfied patient, the peripheral breast tissue had some areas of fibrosis. Her preprocedural core biopsy had also demonstrated a more fibrotic and less cellular tumor.

Follow-up mammograms were available only for the seven patients older than 30 years. These mammograms had an appearance similar to that of the final US pattern (Fig 6), but some were difficult to explain; namely, in patients who had a minimal discernible nodule at mammography, one had a distinct smaller mass at US (Fig 6, *A*), while another had residual ill-defined changes at US (Fig 6, *B*). Two of the patients had a slightly larger area of asymmetric density remaining in that area, one of whom was the patient who had cystic degeneration (Fig 6, *C*).

Among the patients who had a palpable mass prior to treatment of their fibroadenomas (95%, 40 of 42), 12-month follow-up questionnaire data were available regarding 37 fibroadenomas. Of these, 89% (33 of 37) had palpably resolved or were substantially less noticeable to the patient by 12 months after the procedure. Patients and health care providers were very satisfied with the cosmetic outcomes. No apparent skin alteration over the iceball site was noted. There were no cases of "volume reduction" skin depres-

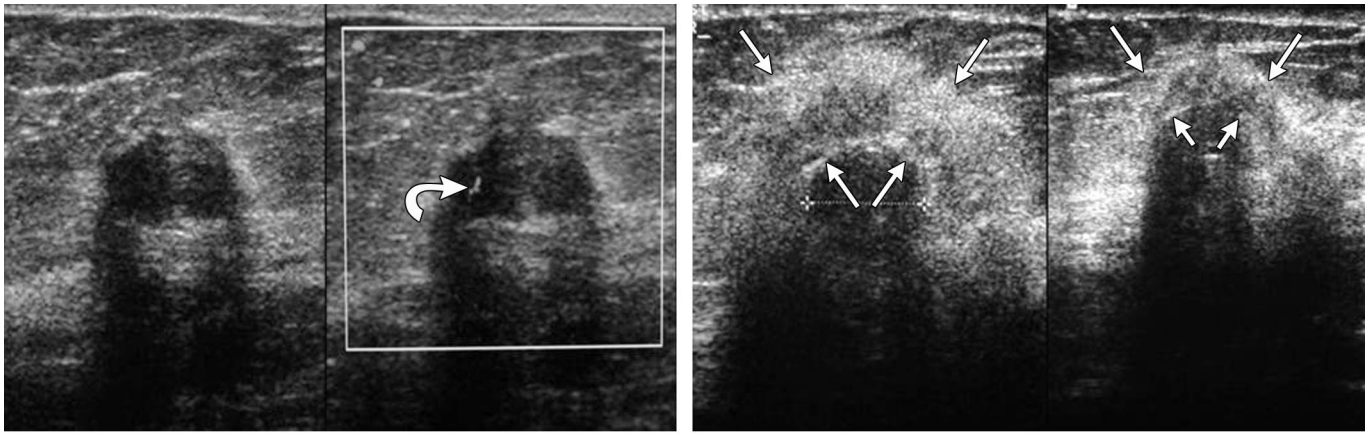

a. b.

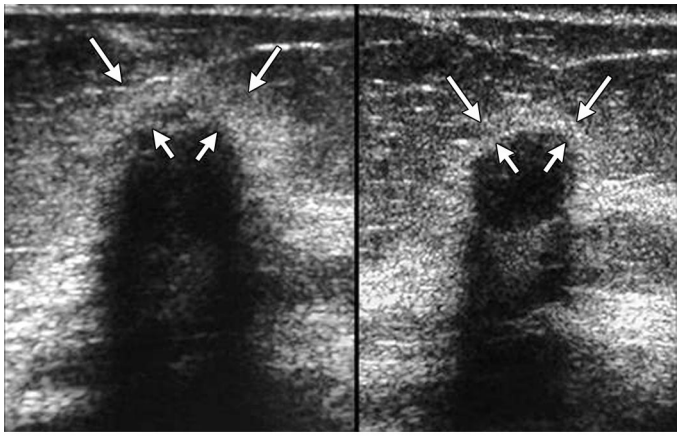

c.

Figure 4. Transverse US images of a fibroadenoma. **(a)** Image with power Doppler view (right) shows only a small amount of internal flow (arrow), common for growing fibroadenomas in our series. **(b)** Images show cryotherapy site at 1 month (left) and 3 months (right) later. Decreasing thickness of adjacent echogenic breast tissue (arrows) most likely corresponds to resolving edematous and/or inflammatory reaction and/or necrosis surrounding the shadowing central fibroadenoma. **(c)** Images show cryotherapy site at 6 (left) and 12 (right) months later. The presumed peripheral organizing necrosis continues to resolve (arrows), as does the central fibroadenoma (decrease of 70%).

sion that can accompany open surgical excision. Scarring at the probe insertion site ranged from complete healing (ie, clinically undetectable) to some hypopigmentation of up to 1.5 cm in three African American patients at 3 months. However, the hypopigmentation resolved at between 6 and 12 months and was attributed to the air-gap–insulated probe. The greatest skin effects were related to different surgical tapes used with the covering gauze pads. Later patients were given only a bandage after the 20-minute compression and were told to place gauze over the bandage and beneath a supportive brassiere to manage any minor immediate oozing. Only one African American patient had a 5-mm hypertrophied scar, or minor keloid formation, at a cryoprobe insertion site. All patients were offered the opportunity to undergo resection of any residual fibroadenoma if they were displeased with the outcome. To date, only two patients have elected to undergo resection (one for a persistent palpable nodule, the other for the previously noted periablational tissue reaction). Several patients displayed their satisfaction by undergoing repeat cryoablation for other fibroadenomas off protocol, once the cryoablation system was approved by the Food and Drug Administration for that indication and became commercially available.

DISCUSSION

Clinical results from our multicenter trial of cryotherapy for breast fibroadenomas have been previously reported (2), and only unique patient features (ie, multiple probes, thermocouples, histologic evaluation) and imaging findings are reported here. The imaging details and characteristics of our patient population are reported in this article to highlight cryobiology principles of selected freeze protocols, available histologic results, longer US imaging outcomes, and potential racial implications. We found the procedure to be easily monitored with US, virtually painless, and highly amenable to a breast clinic or outpatient radiology setting, and it can be performed with only local anesthesia. US also provided reliable follow-up over time, corroborating encouraging clinical outcomes of resolved mass effect and excellent skin cosmesis. Other than transient hypopigmentation at the insertion site, African American patients responded to cryotherapy as well as white patients and showed no evidence of increased keloid formation (17).

Despite common racial trends regarding fibroadenomas and keloids (4–7,18), the most impressive outcome was in a white adolescent who showed nearly complete palpable resolution of seven fibroadenomas treated over an 18-month period (five sessions). She also experienced marked improvement in psychological status and social affect as a result of avoiding contemplated bilateral mastectomies, since she had formed keloids at each of her four resections sites prior to enrolling in this study. Her unusual case (ie, white) still suggests potential connections between benign conditions of altered growth factors. Further work is needed on the etiology of increased fibroadenoma incidence (4–7), keloids (18), and leiomyomata (19) in African-American women, as well as on the potential immune connection of developing fibroadenomas in patients undergoing cyclosporine therapy after transplantation surgery (20). Cryotherapy thus appears

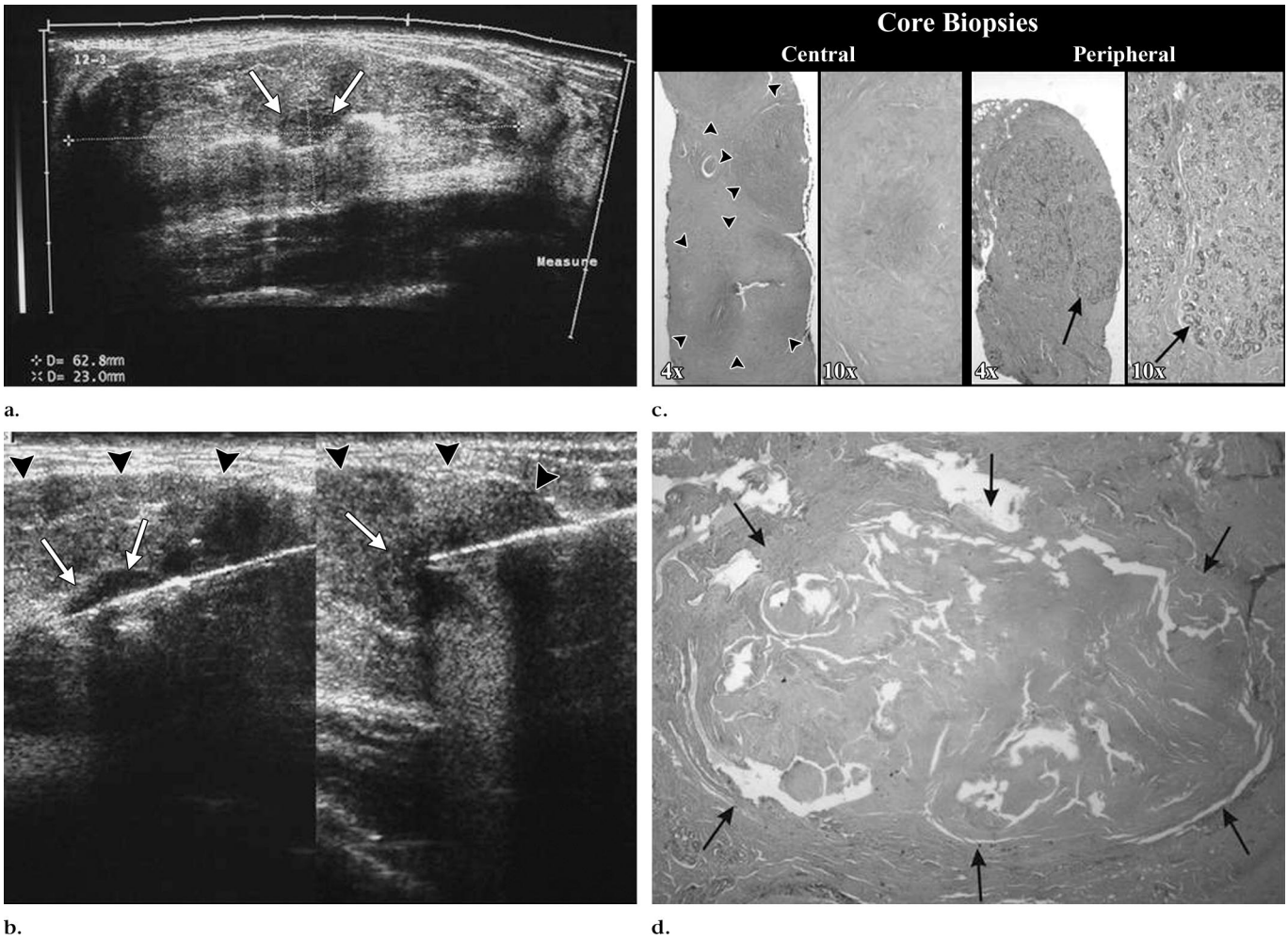

Figure 5. **(a)** US image shows potentially aberrant healing reaction (calipers, 6.3 × 2.3 cm) 6 months after cryotherapy, consisting of a well-circumscribed hypoechoic area surrounding the atrophied fibroadenoma (arrows). **(b)** US image of core biopsy specimens of the central (left) and peripheral (right) components of the healing reaction. Hypoechoic margin of the masslike healing reaction (arrowheads) and shrunken underlying fibroadenoma (arrows) are seen. **(c)** Images of central and peripheral biopsy specimens from **b** at two magnifications. Central biopsy specimens confirm residual whirled architectural pattern of fibroadenoma (×4; arrowheads) replaced by a paucicellular hyaline background (at ×10). Peripheral biopsy specimens show normal parenchyma with glandular epithelium (arrows). (Hematoxlyin-eosin stain). **(d)** Low-magnification whole-specimen view of resected fibroadenoma treatment site (arrows) in the woman who elected to have residual palpable mass effect removed despite US volume reduction (70%). Note acellular central hyaline background without evidence of residual viable fibroadenoma tissue. (Hematoxlyin-eosin stain; original magnification, ×2).

encouraging for special patient groups with multiple and/or growing fibroadenomas.

Important freeze protocol details and equipment differences were not covered in our initial article (2) but can now be better compared (14). Pfleiderer et al (14) documented mean iceball diameters over time by using a 3-mm probe (CryoHit; Galil, Yokneam, Israel) in 16 breast cancers. A notable difference is the speed in achieving a 2.0-cm iceball during the first freeze, which took less than 4 minutes in our series but took approximately 6 minutes with the 3-mm probe in the study by Pfleiderer et al. While the final iceball size of 2.7 cm (after two 7-minute freezes) in that study was similar to our final diameter of approximately 2.9 cm in protocol 3, ours was achieved by using only 4-minute freeze cycles at 100% flow rate. Pfleiderer's group did not record tissue temperatures; they reported only on temperatures from within the probe. In our series, we have shown that thoroughly cytotoxic temperatures (<−40°C) (15–17) occur approximately 5 mm behind the visible second freeze margin during the second freeze and were achieved with faster, more lethal freeze rates. The air-gap–insulated probes used in this study have been replaced by vacuum-insulated trocar-tipped 2.7-mm cryoprobes, eliminating the need for skin protection at the insertion site.

Our clinical success (73% tumor volume reduction and reduction of palpability to acceptable levels in 89% of cases) may relate to a combination of our technique, probe characteristics, short-axis fibroadenoma diameters, and freeze protocols. The protocols used maximal fibroadenoma measurements, yet our technique placed the long axis of the fibroadenoma along the probe shaft to take advantage of the probe's approximately doubled freeze length compared with its width or depth. Therefore, the short-axis diameters of the fibroadenoma are more important for precise tumor targeting than is the overall average diameter. Over-freezing beyond

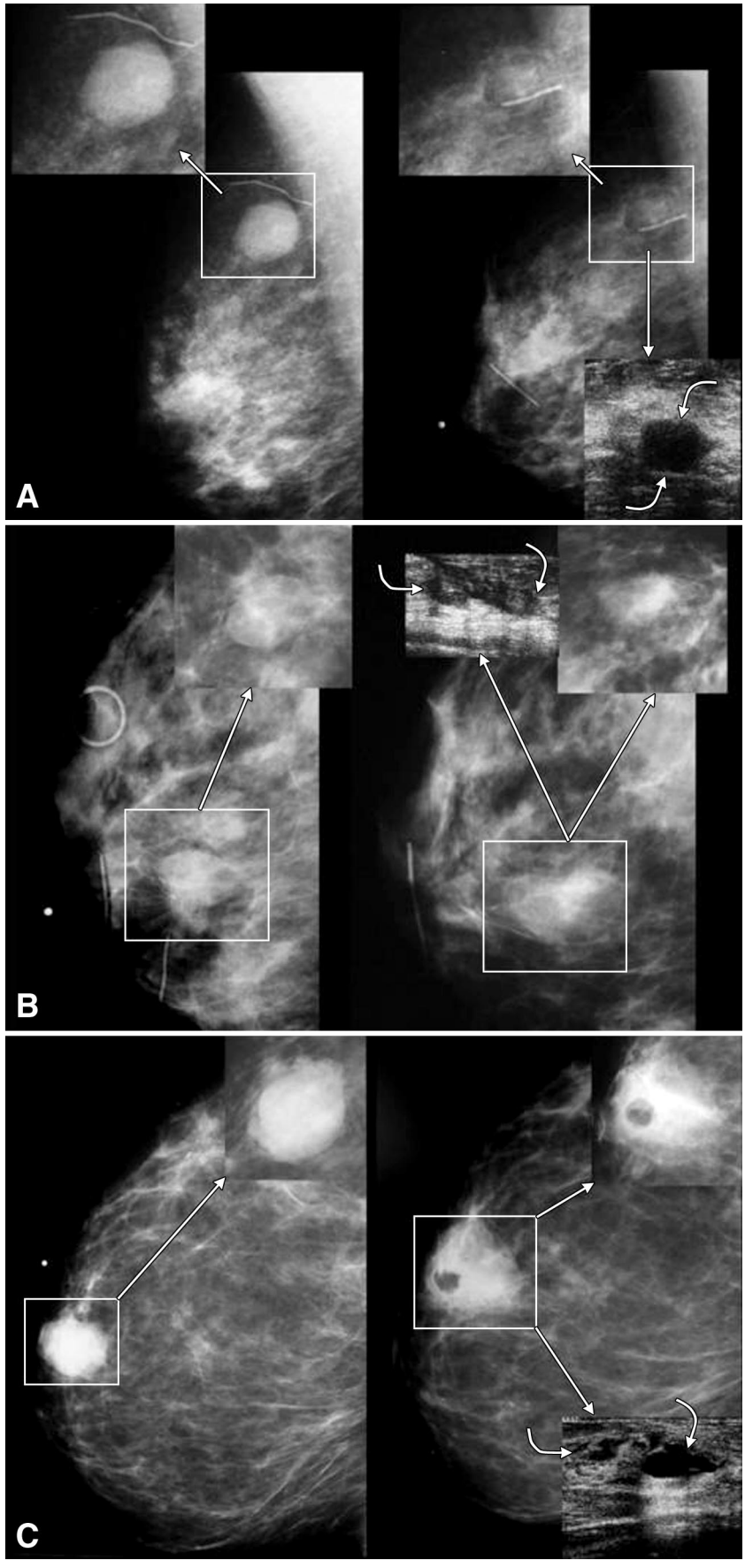

Figure 6. Mammograms with US correlates show changes with cryotherapy at 1 year. *A*, Mediolateral oblique mammograms of 2.5-cm left axillary tail mass before cryotherapy (left) show minimal mass effect after cryotherapy (right); top inset on each image is a magnified view. However, the US image (bottom inset, postcryotherapy image) shows a residual small mass effect (curved arrows). *B*, True lateral mammograms of a distinct central mass within dense breast parenchyma before cryotherapy (left) also shows minimal mass effect after cryotherapy (right), which is better seen in compression views (right inset on each image). The follow-up US image (left inset, postcryotherapy image) only shows ill-defined parenchymal changes (curved arrows). *C*, True lateral mammograms of a 2.8-cm periareolar mass in a fatty breast before cryotherapy (left) show a slightly greater surrounding density after cryotherapy (right), with a central oil cyst; top inset on each image is a magnified view. US image (bottom inset, postcryotherapy image) shows cystic component (curved arrow on right) and adjacent ill-defined parenchymal changes (curved arrow on left).

the limits of the tumor in the longitudinal axis (eg, smaller tumors) and under-freezing in the short axis (eg, larger tumors) may be easily remedied by using newer vacuum-insulated cryoprobes. These will also be modified to have shorter longitudinal freeze dimensions for more spheroid ice that better matches tumor shapes. Probe selection options will allow greater treatment flexibility while lessening the burdens of precise central probe placement in a firm tumor lying within loose breast fat (ie, mobile and operator-dependent). Rapidly advancing cryotechnology will also be crucial for cancer applications that have great potential for breast conservation yet require thorough understanding of cryobiology principles (14).

Many of our patients who had maximal tumor diameters of less than 2 cm ($n = 15$) were adolescents and other nulliparous females, for whom future lactation is a concern. We thus modified our freeze protocol after this trial to reduce excessive necrosis of normal tissue while maintaining aggressive freeze parameters. Rapid dual freezes could minimize the role of the "maintenance" portion of each freeze (16,17). This dual-freeze technique is similar to current prostate freezing protocols that use tightly controlled thermocouple monitoring (15), which has recently progressed to automated control of multiple cryoprobes by way of adjacent thermocouple readings (AutoFreeze, Endocare). Yet the longer a freeze is held near the maximum iceball capac-

ity of each probe, the colder the isotherm becomes at the ice margin (−29°, −38°, −45°C for protocols 2, 3, and 4, respectively).

While we are confident that standardized freeze protocols can work well for less-experienced physicians, we currently emphasize close monitoring with US for all mass sizes. For masses less than 2 cm in short-axis diameter, we rapidly push the ice margin 3–5 mm beyond the fibroadenoma margins at 100% duty cycle, thaw for at least 6 minutes, then rapidly refreeze to even greater ice size. For larger masses that approach the maximal freeze capacity of the cryoprobe (ie, ice expansion slows to "maintenance" rates of approximately 0.1 cm/min), longer freeze times are needed to achieve the expansion of the lethal isotherm, as seen in the later portion of the freeze curves. Larger freezes approaching 3 cm may need to be held for up to 10 minutes each, with an interposed thaw for more than 6 minutes. Alternatively, we also now use a bracketing approach for masses that are 3–4 cm, whereby we place two probes approximately 1.5–2.0 cm apart to allow rapid freezing and to thoroughly cover tumor margins. We recognize that these modifications require greater operator dependence. However, ice monitoring after probe placement is easily seen by using high-frequency (ie, high spatial resolution) linear-array breast US transducers, similar to the exquisite monitoring of hepatic cryotherapy by using intraoperative US (21).

The limited confirmatory tissue from this series corroborates pathologic findings of cryotherapy in other organ systems. Minimal scarring from cryotherapy makes it widely used for many dermatologic conditions (22). The preservation of collagenous architecture in a fibrous target (23) helps explain why postcryotherapy prostates maintain similar shape and size, while biopsy specimens show only a hyaline-replaced matrix (15). Similarly, the lack of perforation and/or destruction of the cartilaginous rings of the bronchial tree by using cryotherapy led some to suggest its superiority over heat-based ablations for endobronchial neoplasms (24). The excellent cosmetic outcome (ie, 80% palpable resolution and minimal skin-puncture site) for patients in our series suggests minimal scarring, with similar architectural preservation of the shrunken fibroadenoma collagen matrix. The lack of satisfactory palpable shrinkage in the one patient who elected to undergo resection may relate in part to the relatively fibrous nature of the pretreatment biopsy specimens (ie, similar to the more fibrous architecture of prostates showing minimal shrinkage). Further work is needed to assess whether hypocellularity in pretreatment biopsy specimens may serve as a prognostic indicator for satisfactory cryotherapy response (ie, is the fibroadenoma more on the "fibro" or the "adenoma" end of the spectrum?).

US also served as a surrogate for histologic response at follow-up. Early increased echogenicity of ablated tissue beyond the fibroadenoma and the early hypervascular rim mostly likely relates to acute edema and an inflammatory infiltrate at those sites (22). The increasingly hypoechoic appearance over time likely represents tissue involution and organization that is similar to a healing hematoma. One patient did have a small cystic area develop within the fragmentation of the primary fibroadenoma by 6 months. This "autofragmentation" phenomenon corresponded to virtual resolution of the palpable area in most patients. The central areas of the fibroadenoma scar on US images also appeared to closely correspond to pathologic measurements of the hyaline replacement in the shrunken collagenous architecture of the former fibroadenoma. While the mammographic data are limited, they suggest a similar overall healing course, with decreased mass effect and no evidence of dystrophic calcifications.

The potential aberrant tissue reactions surrounding the involuted fibroadenoma in three (11%) of 27 patients are difficult to understand in the face of histologic results from biopsy and resection specimens that showed normal surrounding breast parenchyma. We can only postulate an exacerbated healing reaction that may have a complex immunologic, genetic, and/or hormonal basis. Cryoablation zones have a surrounding hypervascular rim, which has been shown to create apoptosis in cells near the periphery that do not die immediately (22). Cells surviving those apoptotic mechanisms may be prone to hyperstimulated growth, whether that is from hormonal, vascular, or other stimuli. The idiosyncratic tissue reactions seen in our patients most likely incorporate several facets of these complex interactions, suggesting both caution and future treatment possibilities for any malignancy. Specifically, cryotherapy for breast cancer requires detailed knowledge of US-driven freezing protocols to avoid under-treatment of tumors larger than 1.5 cm (14). Likewise, the hypervascular rim suggests a potential for enhanced chemotherapy delivery or greater sensitization to radiation. Regardless of the type of image-guided breast cancer treatment, clear definition of tumor margins in relation to treatment margins will be crucial (25). This may require further developments in US to provide clear tissue differentiation (26) and monitor treatment outcomes rather than rely on the costly and limited access of magnetic resonance imaging (27).

Limitations of the current study involve the rapidly developing cryoablation technology and associated technique modifications. During the course of this study, an important cryoablation technology advancement included the vacuum jacket of the cryoprobes, which thereby removed the need for an insertion trocar or associated continuous fluid dripping for skin protection. In addition, it was noted that saline injection was needed only for skin overlying a fibroadenoma, since the underlying pectoralis muscle could be protected by simply elevating the whole probe with gentle to-and-fro movement. The thermocouple monitoring performed for this study was done primarily for definition of freezing protocols to help automate the equipment for physician offices or clinics. However, practicing radiologists will recognize the ease of use in simply monitoring the echogenic iceball as its rim extends 0.5 mm beyond the fibroadenoma margin. The operator dependence of placing the probe within the center of a lesion may be a limitation for less-skilled imagers but also emphasizes the important role of radiologists for this procedure. As cryoablation technology gets applied to breast cancer in the future, the need for thermometry to ensure cytotoxic temperatures beyond well-visualized tumor margins becomes more critical, similar to prostate cryotherapy, in which thorough treatment of even aggressive tumors has been validated (14).

In summary, scarring and cosmesis are not trivial concerns for patients undergoing breast surgery, especially for women with multiple tumors, history of keloid formation, or prior excisions. Cryotherapy of breast fibroadenomas causes minimal discomfort and can provide improved cosmesis with which patients are very satisfied. In addition, costs for treating benign tumors may be reduced by preventing open resection, as well as by treating tumors in an outpatient clinic setting rather than in an ambulatory surgery setting.

Acknowledgment: The authors thank all health care workers associated with the development of breast cryotherapy, specifically Dianna Hatch, BS, ARDMS, for all US coordination and the staff of the Walt Comprehensive Breast Center.

References

1. Medical Data International, vol 7. November-December 1997; 305.
2. Kaufman CS, Bachman B, Littrup PJ, et al. Office-based ultrasound-guided cryoablation of breast fibroadenomas. Am J Surg 2002; 184:394–400.
3. Kaufman CS, Littrup PJ, Freeman-Gibb LA, et al. Office-based cryoablation of breast fibroadenomas: 12-month follow-up. J Am Coll Surg 2004; 198:914–923.
4. Funderburk WW, Rosero E, Leffall LD. Breast lesions in blacks. Surg Gynecol Obstet 1972; 135:58–60.
5. Oluwole SF, Freeman HP. Analysis of benign breast lesions in blacks. Am J Surg 1979; 137:786–789.
6. Organ CH Jr, Organ BC. Fibroadenoma of the female breast: a critical clinical assessment. J Natl Med Assoc 1983; 75:701–704.
7. El-Tamer MB, Song M, Wait RB. Breast masses in African American teenage girls. J Pediatr Surg 1999; 34:1401–1404.
8. Parker SH, Klaus AJ, McWey PJ, et al. Sonographically guided directional vacuum-assisted breast biopsy using a handheld device. AJR Am J Roentgenol 2001; 177:405–408.
9. March DE, Coughlin BF, Barham RB, et al. Breast masses: removal of all US evidence during biopsy by using a handheld vacuum-assisted device—initial experience. Radiology 2003; 227:549–555.
10. Izzo F, Thomas R, Delrio P, et al. Radiofrequency ablation in patients with primary breast carcinoma: a pilot study in 26 patients. Cancer 2001; 92:2036–2044.
11. Singletary SE, Fornage BD, Sneige N, et al. Radiofrequency ablation of early-stage invasive breast tumors: an overview. Cancer J 2002; 8:177–180.
12. Dowlatshahi K, Francescatti DS, Bloom KJ. Laser therapy for small breast cancers. Am J Surg 2002; 184:359–363.
13. Staren ED, Sabel MS, Gianakakis LM, et al. Cryosurgery of breast cancer. Arch Surg 1997; 132:28–33.
14. Pfleiderer SO, Freesmeyer MG, Marx C, Kuhne-Heid R, Schneider A, Kaiser WA. Cryotherapy of breast cancer under ultrasound guidance: initial results and limitations. Eur Radiol 2002; 12:3009–3014.
15. Bahn DK, Lee F, Badalament R, Kumar A, Greski J, Chernick M. Targeted cryoablation of the prostate: 7-year outcomes in the primary treatment of prostate cancer. Urology 2002; 60(suppl 1):3–11.
16. Hong JS, Rubinsky B. Patterns of ice formation in normal and malignant breast tissue. Cryobiology 1994; 31:109–120.
17. Rui J, Tatsutani KN, Dahiya R, Rubinsky B. Effect of thermal variables on human breast cancer in cryosurgery. Breast Cancer Res Treat 1999; 53:185–192.
18. Datubo-Brown DD. Keloids: a review of the literature. Br J Plast Surg 1990; 43:70–77.
19. Kjerulff KH, Langenberg P, Seidman JD, Stolley PD, Guzinski GM. Uterine leiomyomas: racial differences in severity, symptoms and age at diagnosis. J Reprod Med 1996; 41:483–490.
20. Weinstein SP, Orel SG, Collazzo L, Conant EF, Lawton TJ, Czerniecki B. Cyclosporin A–induced fibroadenomas of the breast: report of five cases. Radiology 2001; 220:465–468.
21. Lee FT, Mahvi DM, Chosy SG, et al. Hepatic cryosurgery with intraoperative US guidance. Radiology 1997; 202:624–632.
22. Schacht V, Becker K, Szeimies RM, Abels C. Apoptosis and leucocyte-endothelium interactions contribute to the delayed effects of cryotherapy on tumours in vivo. Arch Dermatol Res 2002; 294:341–348.
23. Littrup PJ, Mody A, Sparschu RA, et al. Prostatic cryotherapy: ultrasonographic and pathologic correlation in the canine model. Urology 1994; 44:175–184.
24. Deygas N, Froudarakis, Ozenne G, Vergnon JM. Cryotherapy in early superficial bronchogenic carcinoma. Chest 2001; 120:26–31.
25. Dowlatshahi K, Francescatti DS, Bloom KJ, et al. Image-guided surgery of small breast cancers. Am J Surg 2001; 182:419–425.
26. Littrup PJ, Duric N, Leach RR Jr, et al. Characterizing tissue with acoustic parameters derived from ultrasound data. Proc SPIE 2002; 4687:354–361.
27. Hynynen K, Pomeroy O, Smith DN, et al. MR imaging-guided focused ultrasound surgery of fibroadenomas in the breast: a feasibility study. Radiology 2001; 219:176–185.